Journal of Ultrafine Grained and Nanostructured Materials
https://jufgnsm.ut.ac.ir
Vol. 54, No.1, June 2021, pp. 112-120
Print ISSN: 2423-6845 Online ISSN: 2423-6837
DOI: 10.22059/jufgnsm.2021.01.12

Nanostructured high-entropy alloys by mechanical alloying: A review of principles and magnetic properties

Sara Daryoush, Hamed Mirzadeh*, Abolghasem Ataie

School of Metallurgy and Materials Engineering, College of Engineering, University of Tehran, Tehran, Iran.

Recieved: 30 March 2021; Accepted: 11 May 2021
** Corresponding author email: hmirzadeh@ut.ac.ir*

ABSTRACT

The principles of nanostructured multicomponent high-entropy alloys (HEAs) processed by mechanical alloying are overviewed. Firstly, the general concepts of HEAs (multi-principal element alloys with ≥5 elements), core effects, and phase formation rules are briefly reviewed. Subsequently, the processing of nanocrystalline and amorphous HEAs by mechanical alloying and the effect of high-energy ball milling parameters are summarized. Finally, the magnetic properties of nanostructured HEAs are critically discussed to infer some general rules. In summary, a higher content of ferromagnetic elements (e.g. Fe, Co, and Ni) normally results in a higher saturation magnetization. The as-milled products with solid solution phases show better soft-magnetic properties compared to the fully amorphous phases, and increasing the amount of the amorphous phase decreases the saturation magnetization. The magnetic properties are also influenced by processing (such as sintering) and thermal history through the alteration of phases and crystallite size.

Keywords: *High-entropy alloys; Mechanical alloying; Magnetic properties; Nanostructures.*

1. Introduction

The idea of one principal element in alloys has been largely substituted by more complex chemical compositions [1-4], where the development of superalloys and stainless steels [5] is the obvious outcome of this strategy. Recently, the high-entropy alloys (HEAs) containing at least five principal elements in an equal or near-equal atomic percentage with no obvious difference between the solute and solvent have been developed, most notably the Cantor alloys [2,3]. The high mixing entropy in these alloys enhances the formation of random solid-solution phases with simple crystal structures. The HEAs show unique mechanical performance and functional physical properties (especially excellent magnetic behavior) as well as high thermal stability, which has led to the current increased interest in processing and application of these alloys. Mechanical alloying is the main solid-state route for processing of HEAs, where its advantages are enhanced solid solubility, room temperature processing without the need of melting, and formation of nanostructures. However, the induced contamination during milling, high propensity of oxidation, and low thermal stability (stability of the phases and the retention of nanocrystallinity) are the main challenging issues [6]. Accordingly, the present work is dedicated to evaluate the magnetic properties of nanostructured HEAs processed by mechanical alloying. The basic concepts, phase selection rules, and core effects are presented in the next section. Afterwards, the

interesting features of mechanical alloying for processing of advanced materials (such as HEAs) are overviewed in the subsequent section. Moreover, recent advances in the magnetic properties of HEAs processed by mechanical alloying are presented in the last section.

2. Principles of high-entropy alloys

The increased configurational entropy of mixing in alloys comprising multiple alloying elements (especially at near-equiatomic concentrations) would counteract the tendency for compound formation. There is a competition for the formation of solid solution and intermetallic compounds. The solid solution can be considered ideal for simplification, and hence, enthalpy of mixing for solid solution (ΔH_{mix}) is zero. Moreover, the competing intermetallic compound can be considered perfectly ordered, and hence, the entropy of mixing for the compound (ΔS_f) is zero. The relative stabilities of the solid solution and intermetallic compound then depend on whether $-T\Delta S_{mix}$ for the solid solution is more negative than ΔH_f for the compound. For the total number of constituent elements of n, based on the molar fraction of each element (c_i), the configurational entropy of mixing per mole (ΔS_{conf}) can be expressed as [6-10]:

$$\Delta S_{\text{conf}} = -R\sum_{i=1}^{n} c_i \ln c_i \quad (1)$$

where R is the gas constant. According to the composition-based definition, HEAs contain at least 5 principal elements, each with an atomic percentage between 5 and 35. Therefore, it is not required for the HEAs to be equiatomic or near-equiatomic. Moreover, minor elements can be added to the HEAs to enhance their various properties. Based on the entropy-based definition, the HEAs have a configurational entropy in a random state larger than 1.5R ($\Delta S_{\text{conf}} \geq 1.5R$), no matter they are single phase or multi phases at room temperature. The configurational entropy of an equimolar quinary random solid solution is ln(5)R = 1.61R, which is considered as the ideal configurational entropy of a 5-element alloy. Since their composition and configurational entropy are close to the lower limits of both definitions, the quaternary equimolar alloys are also usually considered to be HEAs. It is noteworthy that alloys with $1.0R < \Delta S_{\text{conf}} < 1.5R$ can be considered as medium-entropy alloys [6-10].

It was stated above that alloys comprising five or more elements would form single-phase solid solutions. In practice, however, usually multiple intermetallic phases form. Therefore, in addition to the mentioned configurational entropy (Equation 1), other considerations need to be noticed. In this respect, the Ω parameter has been introduced based on Equation 2, where the mixing enthalpy (ΔH_{mix}) and the average melting temperature (T_m) can be also obtained based on Equation 2 [6-10]. Note that ΔH_{mix}^{ij} is the enthalpy of mixing for the binary equiatomic element$_i$ element$_j$ alloy [4]. A larger Ω means a higher probability of forming a single-phase random solid solution [6-10].

$$\Omega = T_m \Delta S_{mix} / \left|\Delta H_{mix}\right|$$

$$\Delta H_{mix} = \sum_{i=1, i\neq j}^{n} 4\Delta H_{mix}^{ij} c_i c_j \quad (2)$$

$$T_m = \sum_{i=1}^{n} c_i (T_m)_i$$

Besides the thermodynamic considerations based on the Ω parameter, the Hume-Rothery rules as the well-known guide to the formation of solid solution alloys have been considered by introducing specific composition-weighted terms for differences in atom radii (δ) and electronegativity, and for an average valence electron concentration (VEC). As the most important parameter, δ can be calculated by Equation 3, in which c_i and r_i are the atomic fraction and the atomic radius, respectively. Moreover, VEC can be calculated by Equation 4, in which VEC_i is the VEC of the i^{th} element.

$$\delta = \sqrt{\sum_{i=1}^{n} c_i (1 - r_i / \bar{r})^2}, \bar{r} = \sum_{i=1}^{n} c_i r_i \quad (3)$$

$$VEC = \sum_{i=1}^{n} c_i VEC_i \quad (4)$$

The parameters δ, ΔH_{mix}, and Ω are usually used to predict the formation of solid solution phases in HEAs. The usual effects of these parameters are summarized in Figure 1. In this respect, $-15 < \Delta H_{mix} < 5$ kJ/mol, $1.1 \leq \Omega$, and $\delta \leq 6.6\%$ favor the formation of the solid-solution phase [6-10]. For instance, based on the results of Pandey et al. [11], ΔH_{mix} of 2.35 kJ/mol was calculated for a CoCrCuFeNi HEA, in which a bcc phase and a small amount of fcc phase formed after 65 h of milling. On the other hand, VEC of an alloy constitutes another critical parameter that can influence the crystallinity of a solid solution phase [12]. HEAs with fcc structure possess a VEC ≥ 8.0,

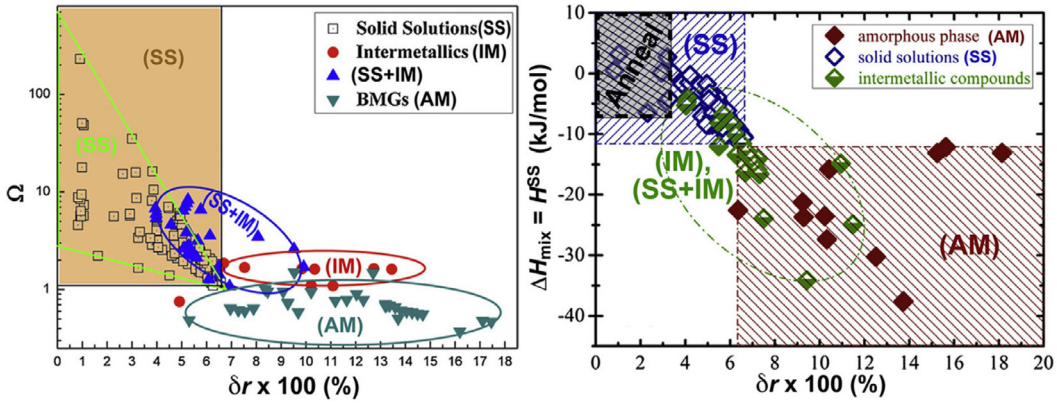

Fig. 1- Empirical correlations to separate phase regions [10]. Note that the as-cast data are typically used, and annealing reduces the extent of the solid solution region.

whereas those with bcc structure possess a VEC < 6.87. When 6.87 ≤ VEC < 8, the stable phase is the coexist of mixed fcc and bcc phases [7,13]. However, while the VEC of the mechanically alloyed Cr-Nb-Ti-V-Zn HEA was calculated as 6.4 suggesting the formation of a bcc phase, a fcc phase was observed, thus violating the VEC principle [14]. In this respect, it has been argued that the non-equilibrium nature of the high energy ball milling process might contribute to the formation of unexpected phases [14,15].

The high-entropy effect (thermodynamics), sluggish diffusion (kinetics), severe lattice distortion (structure), and cocktail effect (properties) are the four core effects for HEAs. The higher mixing entropy in HEAs lowers the free energy of solid solution phases and facilitates their formation, which is known as the high-entropy effect. In HEAs, the neighboring atoms of each lattice site and the diffusion rate of each element is different. Accordingly, the diffusion kinetics in HEAs is sluggish and the kinetics of phase transformations and grain growth are slow due to the need for cooperative diffusion of many kinds of atoms [7,16]. Every atom in the HEAs is surrounded by different kinds of atoms having different atomic sizes, and hence, there is a severe lattice distortion. Moreover, different crystal structure tendencies and bonding energies of constituent elements are expected to enhance the lattice distortion. Therefore, a pronounced solid solution hardening is achieved via impeding of dislocation glide. Moreover, the resultant enhanced scattering of propagating electrons and phonons lowers the electrical and thermal conductivity. The cocktail effect indicates that unusual properties can be obtained after mixing many elements, where the properties of the individual elements as well as their interactions are important [6-10].

3. High-entropy alloys processed by mechanical alloying

Milling of elemental or compound powders is known as mechanical milling (MM); while milling of dissimilar powders is known as mechanical alloying (MA), where the material transfer is involved. The MM process is generally used to reduce the powder particle size, refine the crystallite size (for producing nanostructured materials), and increase the surface area. In addition to the effects mentioned for the MM process, the MA process is also used for alloying and processing of advanced materials. During grinding in a high-energy ball mill, the powder mixture experiences repeated welding, fracturing, and re-welding of powder particles as shown in Figure 2 [17]. Particle flattening (the first stage) results from plastic deformation. This is followed by a welding dominance stage during which the average particle size increases. This effect has been also reported during mechanical alloying of HEAs [18]. During the third stage (equiaxed particle formation), welding and fracturing are rather much in balance and phase lamellae within individual particles are more-or-less parallel. Random welding orientation is the fourth stage. Fracture and welding tendencies are still in balance, but several lamellar colonies exist within each particle. Finally, in the steady-state processing, the layer spacing becomes so fine that it is no longer visible in SEM micrographs and the microstructural refinement continues [17]. Alloying occurs due to the combination

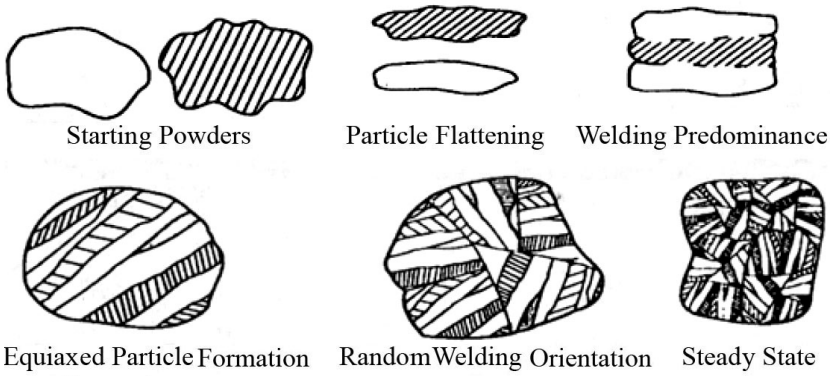

Fig. 2- Stages of powder evolution during mechanical alloying [17].

of decreased diffusion distances (interlamellar spacing), local heating, and increased density of defects [19].

While the stabilization of the solid solution structure is an expected result, the increased configurational entropy in HEAs does not have a significant effect on the dissolution rates during mechanical alloying. For instance, the milling times required to obtain single phase fcc in FeNi is 20 h, while for CoFeNi, CoCrFeNi, and CoCrFeMnNi, it is 15 h [6].

Nanostructured materials can be obtained after sufficient milling time [20-22], as also shown for HEAs [23,24]. The required milling time varies depending on the type of the mill, intensity of milling, ball to powder weight ratio (BPR), and milling temperature [25]. Regarding HEAs, the effects of milling velocity [26] and BPR [27] have been investigated. The energy analysis during mechanical alloying of CuNiCoZnAl HEA showed that the total energy transferred during ball milling was enhanced (1.7 times) by increasing the velocity of ball milling and using balls with different radii [26]. In another study [27], AlCuNiFeCr coatings were successfully synthesized by mechanical alloying technique, where a homogeneous microstructure and improved mechanical properties of the coating layers were obtained at a higher BPR after a long milling duration. For a non-equiatomic FeMnNiCrAlSieC high entropy steel, the crystallite size decreased as the milling time increased, but eventually reached a saturated value [28]. This effect is well-known in mechanical alloying, where an effective milling time for crystallite refinement has been proposed by Mirzadeh and Zomorodian [29].

In fact, milling speed, BPR, milling atmosphere, milling time, milling temperature, and the addition of a process control agent (PCA) are important factors that can affect the mechanical alloying and the characteristics of the resultant powder [30]. At a high BPR, the mean free path of the grinding balls decreases and the number of collisions per unit time increases. More energy is transferred to the powder particles resulting in faster alloying. At high speeds (or intensity of milling) and BPR, i.e. hard milling conditions, the temperature of the vial may reach a relatively high value. This might be advantageous when diffusion is required to promote homogenization and/or alloying. However, increasing the temperature results in the increased crystallite size, leads to the decomposition of supersaturated solid solutions (or other metastable phases), and increases the contamination level of the powder [19]. For instance, in a 40-h milled AlCoCrFeNiTi HEA powder, a single phase bcc phase was observed along with the minor tungsten carbide (WC) phase that formed due to the contamination during milling [31].

The PCA materials as lubricants or surfactants can be solid, liquid, or gaseous. They are mostly organic compounds (such as stearic acid and ethanol) and added at a level of 1–5 wt.% of the powder charge [19]. The adsorption on the metal surface and the lubricating function provided by these molecules are important during mechanical alloying. The former prevents the clean metal-to-metal contact necessary for cold welding, whereas the latter reduces the degree of plastic deformation of powder particles during each impact, which, in turn, slows down the grain refinement process and the formation of solid solutions. The powder yield increases and particle size decreases considerably with addition of PCA during milling as shown by Rabiee et al. [30]. For instance, during mechanical alloying of TiZrNbTa refractory HEA [32], it was

revealed that the liquid PCAs effectively mitigated cold welding. In another investigation [33], it was revealed that PCA can alter the morphology of the HEA powder. The MoNbTaW HEA powders prepared with stearic acid and without any PCAs had a near-spherical shape, while alcohol led to a lamellar morphology.

Murty and co-workers were the first researchers that produced nanocrystalline HEAs by mechanical alloying [34,35]. The processing of HEAs by mechanical alloying results in the development of nanostructured microstructures [36]. For instance, nanocrystalline bcc solid solution during mechanical alloying of WMoNbZrV with average crystallite size of 10 nm, lattice strain of 0.58% and lattice parameter of 3.1687 Å was obtained by Oleszak et al [23]. Heating the sample up to 700 °C resulted in decrease of lattice strain down to 0.20%, while the crystallite size remained unchanged, testifying good thermal stability of the nanocrystalline bcc solid solution obtained [23]. An equiatomic nanocrystalline AlCoCrFeNi HEA was synthesized by Shivam et al. [37] via mechanical alloying route. Milled powder after 30 h showed good chemical homogeneity and refined morphology with a mean particle size of ~ 4 μm. Solid solution phase with bcc crystal structure was confirmed in the as-synthesized HEA. However, the milled alloy powder was not thermally stable, leading to a combination of high entropy and medium entropy phases in the annealed condition [37].

Nanocomposites can be obtained by mechanical alloying [38-44]. In this respect, the processing of high-entropy nanocomposites has received a considerable attention in recent years [45]. For instance CoCrFeMnNi composite with 5% additions of Al_2O_3 nano-particles was produced by mechanical alloying and consolidation by hot isostatic pressing (HIP). The predominant presence of fcc solid solution with aluminum oxide and small amount of $M_{23}C_6$ carbides was characterized [46]. The formation of nanoparticles-woven architectural structures consisting of externally-added SiC nanoparticles between neighboring grains and the in-situ formed $M_{23}C_6$ nanocarbides were observed in a mechanically alloyed and spark plasma sintering (SPS) treated $Fe_{40}Mn_{40}Cr_{10}Co_{10}$/SiC medium-entropy nanocomposite [47]. In another study, TiO(C) nanoparticles in the $CoCrFeNiMnTi_{0.15}$ alloy made the fcc matrix grains clearly finer than those in the $CoCrFeNiMnNb_{0.1}$ sample with NbC and $(Cr,Mn)_3O_4$ nanoparticles [48], which indicates the advantage of particles in this HEA.

Amorphous materials can be obtained by mechanical alloying, where the XRD amorphization parameter has been recently proposed by Adelfar et al. [49,50] and successfully used for amorphization and crystallization studies. The processing of amorphous high-entropy alloys by mechanical alloying has been studied recently. For instance, the amorphization behavior of $Zr_xFeNiSi_{0.4}B_{0.6}$ HEAs by mechanical alloying has been studied [51], where by increasing Zr ratio, the time of complete amorphous phase formation was shortened. This in turn enhanced the amorphization ability. The $ZrFeNiSi_{0.4}B_{0.6}$ and $Zr_{1.5}FeNiSi_{0.4}B_{0.6}$ HEA powders were partially amorphous but still retained the stable fcc solid solution structure. However, the $Zr_{2.5}FeNiSi_{0.4}B_{0.6}$ pseudo HEA powder obtained full amorphous structure after milling for 180 h and gained a high thermal stability [51]. Amorphous powder molding via mechanical alloying and ultrahigh pressure consolidation was considered as a viable processing route to obtain an optimal microstructure of amorphous structure with nanoparticles uniformly distributed in the matrix. This approach can effectively inhibit the crystallization of amorphous structure, thus providing a pathway for manufacturing next-generation non-equiatomic high-entropy metallic glasses [52].

4. Magnetic Properties of mechanically alloyed high-entropy alloys

The presence of the ferromagnetic Fe, Co, and Ni in the chemical composition of notable HEAs resulted in the recent interest in studying their magnetic properties [53]. A higher content of these elements normally results in a higher saturation magnetization (M_s). However, the amount and distribution of the anti-ferromagnetic Cr can have a significant effect, where the addition of 25 % Cr to the CoFeNi alloy makes the CoCrFeNi alloy paramagnetic [7]. Moreover, the reported coercivities (H_c) are usually less than 100 Oe, while some HEAs have higher values ranging from 250 to about 400 Oe [7]. It should be noted that ferromagnetic materials form permanent magnets, or are attracted to magnets, while paramagnetic ones are weakly attracted by an externally applied magnetic field, and form internal, induced magnetic fields in the direction of the applied magnetic

field. Moreover, M_s is a measure of the maximum amount of field that can be generated by a material. Furthermore, H_c is a measure of the ability of a ferromagnetic material to withstand an external magnetic field without becoming demagnetized. Hard magnets have a strong coercivity and are typically used as permanent magnets. On the other hand, magnets with weak coercivity are called soft magnets [54,55].

Regarding HEAs processed by mechanical alloying, the as-milled products with solid solution phases show better soft-magnetic properties compared to the fully amorphous phases [7]. For instance, for the mechanically alloyed equi-atomic FeSiBAlNi(Nb) HEAs, the as-milled powder was soft magnetic with low H_c, and M_s decreased at long milling times mainly due to the amorphization (Figure 3) [56]. In another study on the FeSiBAlNi system, the co-existence of the fcc and bcc phases gave rise to a higher M_s compared to the single amorphous phase or mixture of amorphous and fcc phases [57]. Moreover, Co, Cu, and Ce additions to FeSiBAlNi system obviously shortened the formation time of fully amorphous phase, and hence, decreased the value of M_s as shown in Figure 4 [57,58].

Generally, the initial composition, atomic-scale structure, and the phase constitution are the primary factors in determining the M_s of alloys powders. On the other hand, the grain size and impurity are the main influencing factors on H_c [59]. For instance, as shown in Figure 5, the mechanically alloyed FeCoNiCuAl HEA possesses high M_s and low H_c showing soft magnetic characteristics. The decrease of M_s on increasing milling time can be related to the more intense dissolution of non-ferromagnetic powders (Cu and Al) into ferromagnetic powders (Fe, Co and Ni) [59].

The effects of alloying elements might be significant. For instance, the magnetic properties of the mechanically alloyed $CoCr_xCuFeMnNi$ HEAs versus Cr content are summarized in Figure 6. It can be seen that the soft magnetic properties degraded with the increase of Cr content. The increase of Cr content can decrease the content of ferromagnetic components, leading to the decreased M_s. On the other hand, the fcc phase has a higher M_s compared to the bcc phase, and by increasing Cr content, the phase structure transforms to a mixed structure of bcc and fcc phases from the single fcc phase [60]. Expectedly, the improvement of the soft magnetic properties of the $Co_xCrCuFeMnNi$ HEA powders by increasing the Co content has been reported [61].

The magnetic properties are also influenced by processing and thermal history through the alteration of phases [62-64]. For instance, the formation of a single-phase solid solution of bcc structure was observed in an equiatomic AlCoCrFeNi HEA after 30 h of milling. Subsequent

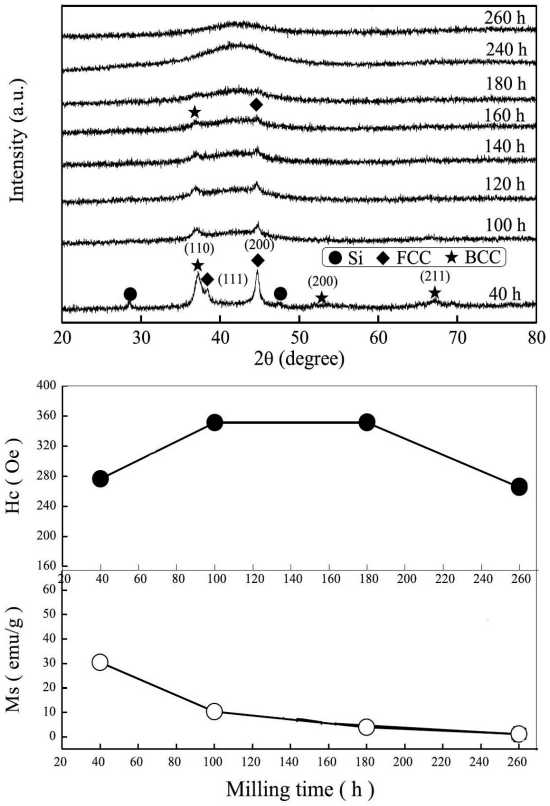

Fig. 3- XRD patterns and magnetic properties of the as-milled FeSiBAlNi(Nb) HEA powders after different milling times [56].

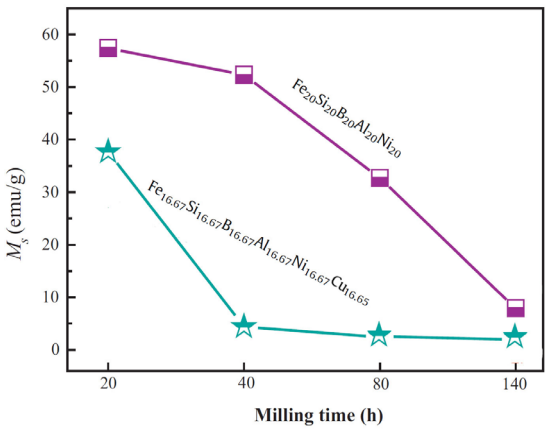

Fig. 4- Saturation magnetization of the as-milled FeSiBAlNi(Cu) HEA powders after different milling times [57].

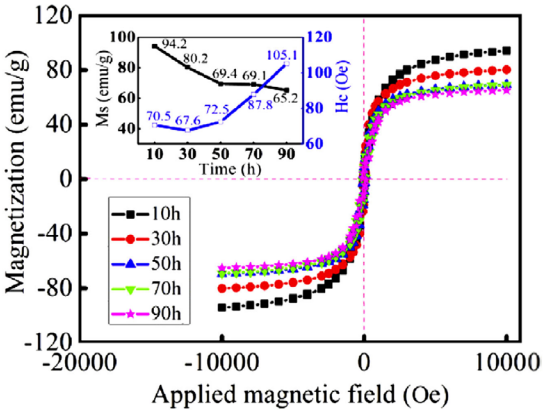

Fig. 5- Hysteresis loops of FeCoNiCuAl HEA powders of the as-milled powders after different milling times [59].

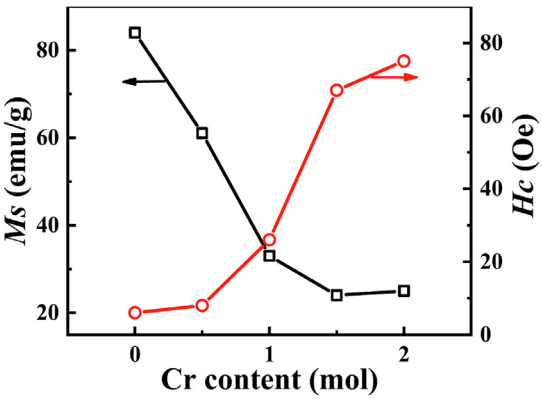

Fig. 6- Magnetic properties of the mechanically alloyed $CoCr_xCuFeMnNi$ HEA powders [60].

sintering led to a phase transition from the parent bcc phase to Ni-Al type B2 and Ni_3Al type $L1_2$ phase, where the M_s of 30 h milled powder and sintered AlCoCrFeNi HEA turns out to be 47.7 and 70.05 emu/g, respectively. Higher values of saturation magnetization in the sintered sample were related to the grain coarsening, more crystallinity and the phase transformation from a single phase to a two-phase structure [64].

5. Summary

In summary, the general concepts related to HEAs and phase formation rules were briefly reviewed in the first part of this overview. Subsequently, the processing of HEAs by mechanical alloying and the effect of high-energy ball milling parameters were summarized. Finally, the magnetic properties of nanostructured HEAs were critically discussed to infer some general rules. It was revealed that a higher content of ferromagnetic elements (e.g. Fe, Co, and Ni) normally results in a higher saturation magnetization. The as-milled products with solid solution phases show better soft-magnetic properties compared to the fully amorphous phases, and hence, increasing the amount of the amorphous phase decreases the saturation magnetization. The magnetic properties are also influenced by processing (such as sintering) and thermal history through the alteration of phases and grain coarsening.

References

1. Pandey VK, Shadangi Y, Shivam V, Basu J, Chattopadhyay K, Majumdar B, et al. Synthesis, Characterization and Thermal Stability of Nanocrystalline MgAlMnFeCu Low-Density High-Entropy Alloy. Transactions of the Indian Institute of Metals. 2020;74(1):33-44.
2. Cantor B, Chang ITH, Knight P, Vincent AJB. Microstructural development in equiatomic multicomponent alloys. Materials Science and Engineering: A. 2004;375-377:213-8.
3. Yeh JW, Chen SK, Lin SJ, Gan JY, Chin TS, Shun TT, et al. Nanostructured High-Entropy Alloys with Multiple Principal Elements: Novel Alloy Design Concepts and Outcomes. Advanced Engineering Materials. 2004;6(5):299-303.
4. Takeuchi A, Inoue A. Classification of Bulk Metallic Glasses by Atomic Size Difference, Heat of Mixing and Period of Constituent Elements and Its Application to Characterization of the Main Alloying Element. MATERIALS TRANSACTIONS. 2005;46(12):2817-29.
5. Soleimani M, Kalhor A, Mirzadeh H. Transformation-induced plasticity (TRIP) in advanced steels: A review. Materials Science and Engineering: A. 2020;795:140023.
6. Vaidya M, Muralikrishna GM, Murty BS. High-entropy alloys by mechanical alloying: A review. Journal of Materials Research. 2019;34(5):664-86.
7. High-Entropy Alloys. Springer International Publishing; 2016.
8. George EP, Raabe D, Ritchie RO. High-entropy alloys. Nature Reviews Materials. 2019;4(8):515-34.
9. Zhang Y, Zhou YJ, Lin JP, Chen GL, Liaw PK. Solid-Solution Phase Formation Rules for Multi-component Alloys. Advanced Engineering Materials. 2008;10(6):534-8.
10. Miracle DB, Senkov ON. A critical review of high entropy alloys and related concepts. Acta Materialia. 2017;122:448-511.
11. Pandey VK, Shivam V, Sarma BN, Mukhopadhyay NK. Phase evolution and thermal stability of mechanically alloyed CoCrCuFeNi high entropy alloy. Materials Research Express. 2020;6(12):1265b9.
12. Ye YF, Wang Q, Lu J, Liu CT, Yang Y. High-entropy alloy: challenges and prospects. Materials Today. 2016;19(6):349-62.
13. Guo S, Ng C, Lu J, Liu CT. Effect of valence electron concentration on stability of fcc or bcc phase in high entropy alloys. Journal of Applied Physics. 2011;109(10):103505.
14. Dwivedi A, Koch CC, Rajulapati KV. On the single phase fcc solid solution in nanocrystalline Cr-Nb-Ti-V-Zn high-entropy alloy. Materials Letters. 2016;183:44-7.
15. Shivam V, Sanjana V, Mukhopadhyay NK. Phase Evolution and Thermal Stability of Mechanically Alloyed AlCrFeCoNiZn

High-Entropy Alloy. Transactions of the Indian Institute of Metals. 2020;73(3):821-30.
16. Najafkhani F, Kheiri S, Pourbahari B, Mirzadeh H. Recent advances in the kinetics of normal/abnormal grain growth: a review. Archives of Civil and Mechanical Engineering. 2021;21(1).
17. Maurice D, Courtney TH. Modeling of mechanical alloying: Part III. Applications of computational programs. Metallurgical and Materials Transactions A. 1995;26(9):2437-44.
18. Tian L, Fu M, Xiong W. Microstructural Evolution of AlCoCrFeNiSi High-Entropy Alloy Powder during Mechanical Alloying and Its Coating Performance. Materials (Basel). 2018;11(2):320.
19. Suryanarayana C. Mechanical Alloying and Milling Marcel Dekker. EE. UU. 2004.
20. Amiri Talischi L, Samadi A. Structural characterization and ordering transformation of mechanically alloyed nanocrystalline Fe-28Al powder. Journal of Ultrafine Grained and Nanostructured Materials. 2016 Dec 1;49(2):112-9.
21. Shahsavari E, Zamani C, Ahmadi Dermeni H, Hadian AM, Hadian A. Cryomilling-Assisted Synthesis of Nanostructured Silicon. Journal of Ultrafine Grained and Nanostructured Materials. 2020 Dec 28;53(2):158-65.
22. Haghighat-Shishavan S, Kashani Bozorg F. Nano-Crystalline Mg (2-x) MnxNi Compounds Synthesized by Mechanical Alloying: Microstructure and Electrochemistry. Journal of Ultrafine Grained and Nanostructured Materials. 2014 Jun 1;47(1):43-9.
23. Oleszak D, Antolak-Dudka A, Kulik T. High entropy multicomponent WMoNbZrV alloy processed by mechanical alloying. Materials Letters. 2018;232:160-2.
24. Maulik O, Kumar D, Kumar S, Fabijanic DM, Kumar V. Structural evolution of spark plasma sintered AlFeCuCrMgx (x = 0, 0.5, 1, 1.7) high entropy alloys. Intermetallics. 2016;77:46-56.
25. Enayati MH, Mohamed FA. Application of mechanical alloying/milling for synthesis of nanocrystalline and amorphous materials. International Materials Reviews. 2014;59(7):394-416.
26. Salemi F, Abbasi MH, Karimzadeh F. Synthesis and thermodynamic analysis of nanostructured CuNiCoZnAl high entropy alloy produced by mechanical alloying. Journal of Alloys and Compounds. 2016;685:278-86.
27. Chen C-L, Suprianto. Microstructure and mechanical properties of AlCuNiFeCr high entropy alloy coatings by mechanical alloying. Surface and Coatings Technology. 2020;386:125443.
28. Jain H, Shadangi Y, Shivam V, Chakravarty D, Mukhopadhyay NK, Kumar D. Phase evolution and mechanical properties of non-equiatomic Fe–Mn–Ni–Cr–Al–Si–C high entropy steel. Journal of Alloys and Compounds. 2020;834:155013.
29. Mirzadeh H, Zomorodian A. Ball milling criteria for producing nano intermetallic compounds. Materials Science and Technology. 2010;26(3):281-4.
30. Rabiee M, Mirzadeh H, Ataie A. Unraveling the effects of process control agents on mechanical alloying of nanostructured Cu-Fe alloy. Journal of Ultrafine Grained and Nanostructured Materials. 2016 Jun 1;49(1):17-21.
31. Shivam V, Shadangi Y, Basu J, Mukhopadhyay NK. Alloying behavior and thermal stability of mechanically alloyed nano AlCoCrFeNiTi high-entropy alloy. Journal of Materials Research. 2019;34(5):787-95.
32. Qiao Y, Tang Y, Li S, Ye Y, Liu X, Zhu La, et al. Preparation of TiZrNbTa refractory high-entropy alloy powder by mechanical alloying with liquid process control agents. Intermetallics. 2020;126:106900.
33. Tong Y, Qi P, Liang X, Chen Y, Hu Y, Hu Z. Different-Shaped Ultrafine MoNbTaW HEA Powders Prepared via Mechanical Alloying. Materials (Basel). 2018;11(7):1250.
34. Varalakshmi S, Kamaraj M, Murty BS. Synthesis and characterization of nanocrystalline AlFeTiCrZnCu high entropy solid solution by mechanical alloying. Journal of Alloys and Compounds. 2008;460(1-2):253-7.
35. Vaidya M, Karati A, Marshal A, Pradeep KG, Murty BS. Phase evolution and stability of nanocrystalline CoCrFeNi and CoCrFeMnNi high entropy alloys. Journal of Alloys and Compounds. 2019;770:1004-15.
36. Koch CC. Nanocrystalline high-entropy alloys. Journal of Materials Research. 2017;32(18):3435-44.
37. Shivam V, Basu J, Pandey VK, Shadangi Y, Mukhopadhyay NK. Alloying behaviour, thermal stability and phase evolution in quinary AlCoCrFeNi high entropy alloy. Advanced Powder Technology. 2018;29(9):2221-30.
38. Rabiee M, Mirzadeh H, Ataie A. Processing of Cu-Fe and Cu-Fe-SiC nanocomposites by mechanical alloying. Advanced Powder Technology. 2017 Aug 1;28(8):1882-7.
39. Rabiee M, Mirzadeh H, Ataie A. Mechanical alloying and consolidation of copper-iron-silicon carbide nanocomposites. Materialwissenschaft und Werkstofftechnik. 2020;51(12):1700-4.
40. Mahdikhah V, Ataie A, Babaei A, Sheibani S, Ow-Yang CW, Abkenar SK. CoFe2O4/Fe magnetic nanocomposite: Exchange coupling behavior and microwave absorbing property. Ceramics International. 2020;46(11):17903-16.
41. Ghorbani A, Sheibani S, Ataie A. Microstructure and mechanical properties of consolidated Cu-Cr-CNT nanocomposite prepared via powder metallurgy. Journal of Alloys and Compounds. 2018;732:818-27.
42. Anvari SZ, Enayati MH, Karimzadeh F. Wear Behavior of Nanostructured Al-Al3V and Al-(Al3V-Al2O3) Composites Fabricated by Mechanical Alloying and Hot Extrusion. Journal of Ultrafine Grained and Nanostructured Materials. 2020 Dec 28;53(2):135-45.
43. Zeraati M, Khayati GR. Optimization of micro hardness of nanostructure Cu-Cr-Zr alloys prepared by the mechanical alloying using artificial neural networks and genetic algorithm. Journal of Ultrafine Grained and Nanostructured Materials. 2018 Dec 1;51(2):183-92.
44. Maddah M, Rajabi M, Rabiee SM. Hydrogen Desorption Properties of Nanocrystalline MgH2-10 wt.% ZrB2 Composite Prepared by Mechanical Alloying. Journal of Ultrafine Grained and Nanostructured Materials. 2014 Jun 1;47(1):21-6.
45. Shadangi Y, Shivam V, Varalakshmi S, Basu J, Chattopadhyay K, Majumdar B, et al. Mechanically driven structural transformation in Sn reinforced Al–Cu–Fe quasicrystalline matrix nanocomposite. Journal of Alloys and Compounds. 2020;834:155065.
46. Rogal Ł, Kalita D, Litynska-Dobrzynska L. CoCrFeMnNi high entropy alloy matrix nanocomposite with addition of Al 2 O 3. Intermetallics. 2017;86:104-9.
47. Wang J, Yang H, Liu Z, Ji S, Li R, Ruan J. A novel Fe40Mn40Cr10Co10/SiC medium-entropy nanocomposite reinforced by the nanoparticles-woven architectural structures. Journal of Alloys and Compounds. 2019;772:272-9.
48. Xie Y, Luo Y, Xia T, Zeng W, Wang J, Liang J, et al. Grain growth and strengthening mechanisms of ultrafine-grained CoCrFeNiMn high entropy alloy matrix nanocomposites fabricated by powder metallurgy. Journal of Alloys and Compounds. 2020;819:152937.
49. Adelfar R, Mirzadeh H, Ataie A, Malekan M. Amorphization and mechano-crystallization of high-energy ball milled Fe Ti alloys. Journal of Non-Crystalline Solids. 2019;520:119466.

50. Adelfar R, Mirzadeh H, Ataie A, Malekan M. Crystallization kinetics of mechanically alloyed amorphous Fe-Ti alloys during annealing. Advanced Powder Technology. 2020;31(8):3215-21.
51. Sang L, Xu Y. Amorphous behavior of ZrxFeNiSi0. 4B0. 6 high entropy alloys synthesized by mechanical alloying. Journal of Non-Crystalline Solids. 2020 Feb 15;530:119854.
52. Yang X, Zhou Y, Zhu R, Xi S, He C, Wu H, et al. A Novel, Amorphous, Non-equiatomic FeCrAlCuNiSi High-Entropy Alloy with Exceptional Corrosion Resistance and Mechanical Properties. Acta Metallurgica Sinica (English Letters). 2019;33(8):1057-63.
53. Zhang Y, Zuo T, Cheng Y, Liaw PK. High-entropy alloys with high saturation magnetization, electrical resistivity, and malleability. Scientific reports. 2013;3:1455-.
54. https://en.wikipedia.org/wiki/Ferromagnetism
55.https://idealmagnetsolutions.com/knowledge-base/coercivity
56. Wang J, Zheng Z, Xu J, Wang Y. Microstructure and magnetic properties of mechanically alloyed FeSiBAlNi (Nb) high entropy alloys. Journal of Magnetism and Magnetic Materials. 2014;355:58-64.
57. Xu J, Shang C, Ge W, Jia H, Liaw PK, Wang Y. Effects of elemental addition on the microstructure, thermal stability, and magnetic properties of the mechanically alloyed FeSiBAlNi high entropy alloys. Advanced Powder Technology. 2016;27(4):1418-26.
58. Xu J, Axinte E, Zhao Z, Wang Y. Effect of C and Ce addition on the microstructure and magnetic property of the mechanically alloyed FeSiBAlNi high entropy alloys. Journal of Magnetism and Magnetic Materials. 2016;414:59-68.
59. Duan Y, Cui Y, Zhang B, Ma G, Tongmin W. A novel microwave absorber of FeCoNiCuAl high-entropy alloy powders: Adjusting electromagnetic performance by ball milling time and annealing. Journal of Alloys and Compounds. 2019;773:194-201.
60. Zhao R-F, Ren B, Zhang G-P, Liu Z-X, Cai B, Zhang J-j. CoCrxCuFeMnNi high-entropy alloy powders with superior soft magnetic properties. Journal of Magnetism and Magnetic Materials. 2019;491:165574.
61. Zhao R-F, Ren B, Zhang G-P, Liu Z-X, Zhang J-j. Effect of Co content on the phase transition and magnetic properties of Co CrCuFeMnNi high-entropy alloy powders. Journal of Magnetism and Magnetic Materials. 2018;468:14-24.
62. Zhu X, Zhou X, Yu S, Wei C, Xu J, Wang Y. Effects of annealing on the microstructure and magnetic property of the mechanically alloyed FeSiBAlNiM (M=Co, Cu, Ag) amorphous high entropy alloys. Journal of Magnetism and Magnetic Materials. 2017;430:59-64.
63. Mishra RK, Shahi RR. Effect of annealing conditions and temperatures on phase formation and magnetic behaviour of CrFeMnNiTi high entropy alloy. Journal of Magnetism and Magnetic Materials. 2018;465:169-75.
64. Shivam V, Shadangi Y, Basu J, Mukhopadhyay NK. Evolution of phases, hardness and magnetic properties of AlCoCrFeNi high entropy alloy processed by mechanical alloying. Journal of Alloys and Compounds. 2020;832:154826.